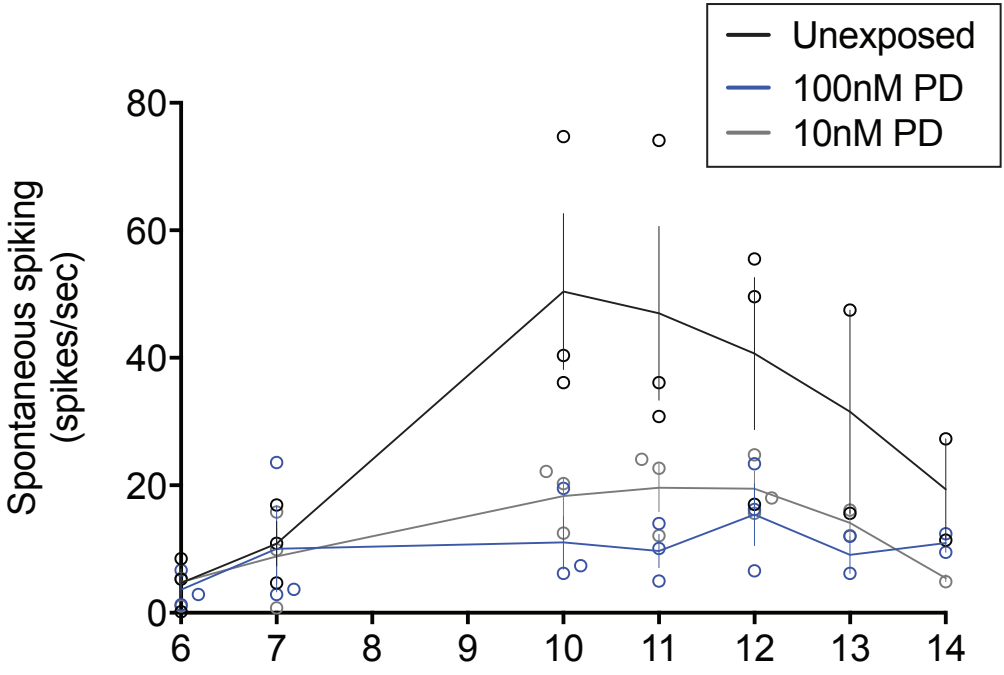

P-value:	6	7	8	9	10	11	12	13	14
Un.-100nM	0.91	0.93	-	-	<0.01 **	<0.01 **	0.01 *	0.10	0.45
Un.-10nM	0.99	0.83	-	-	<0.01 **	<0.01 **	0.02 *	0.12	0.22

Poston et al. Supplementary Figure 1

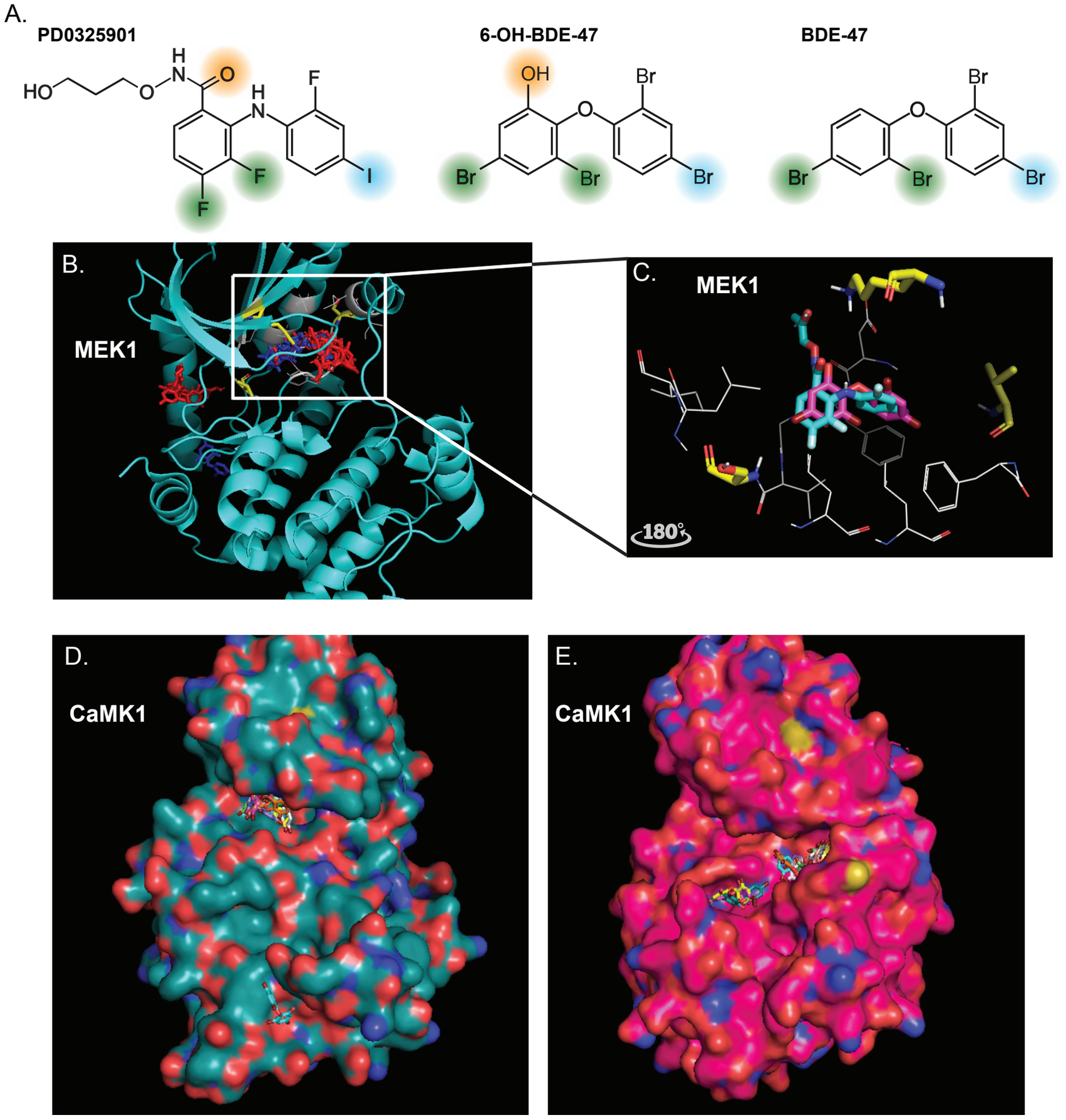

Poston et al. Supplementary Figure 2

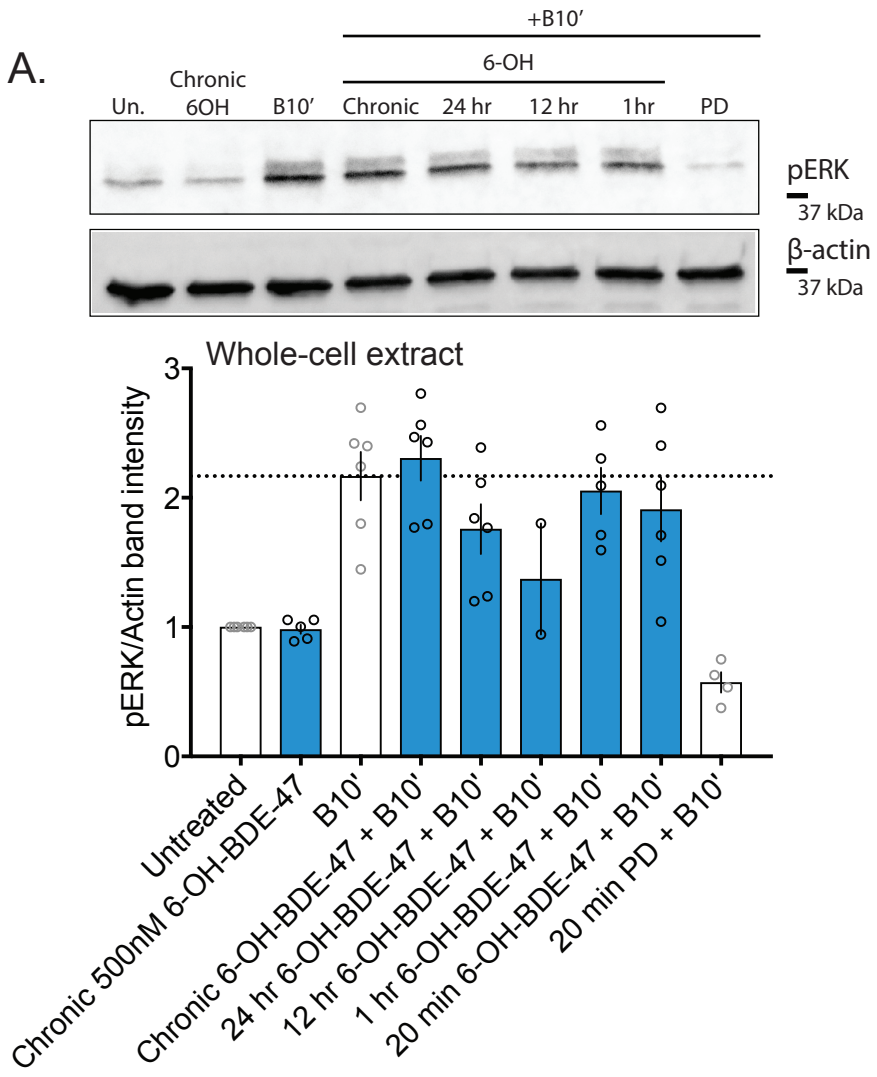

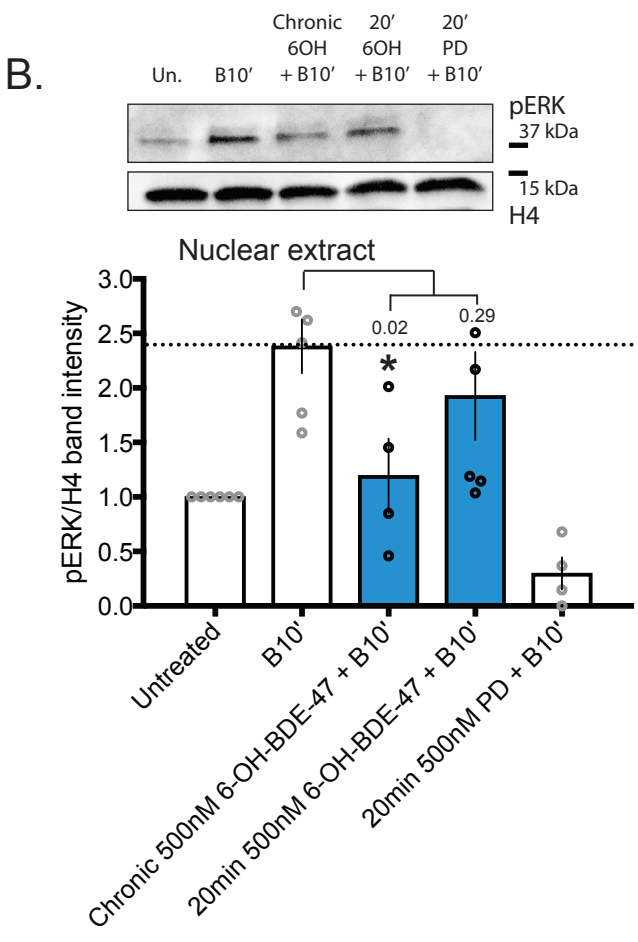

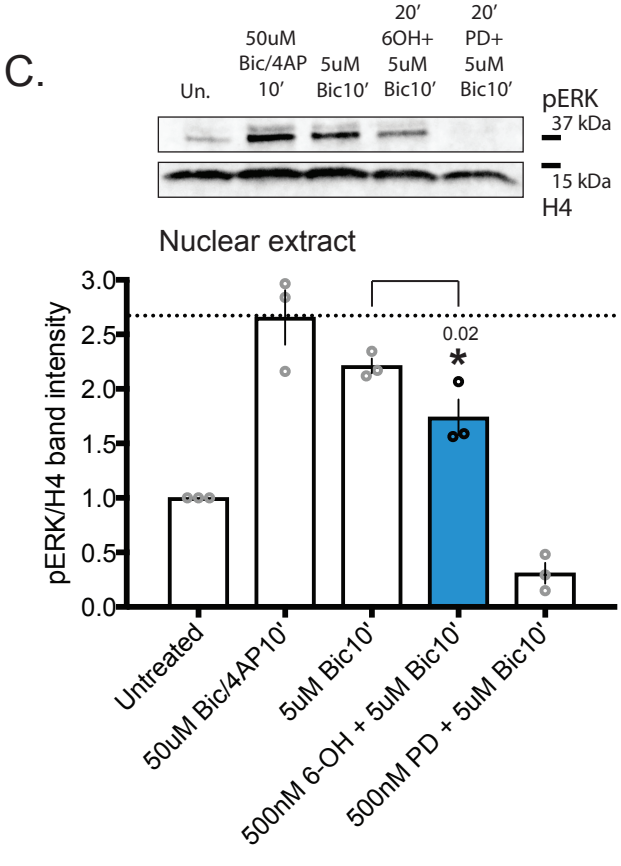

Poston et al. Supplementary Figure 3

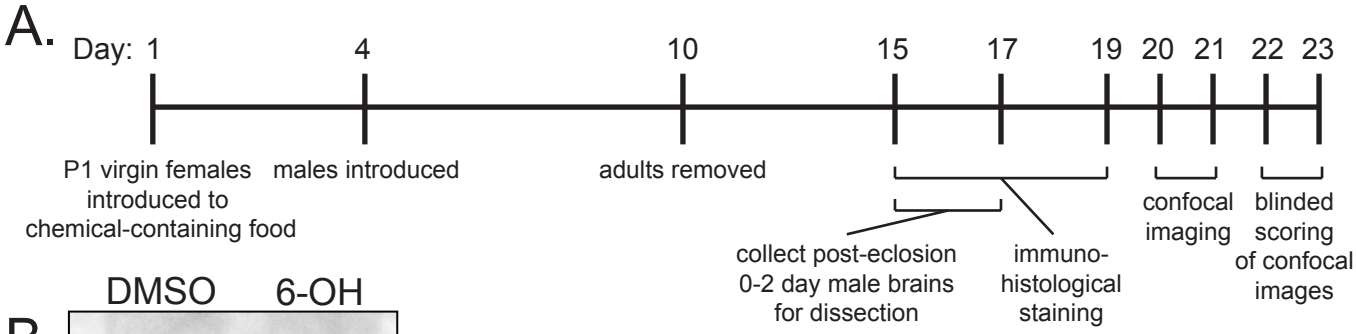

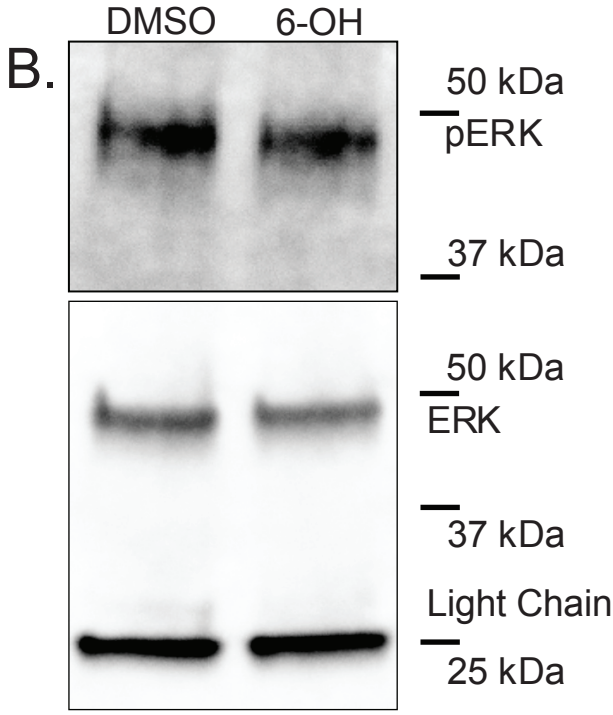

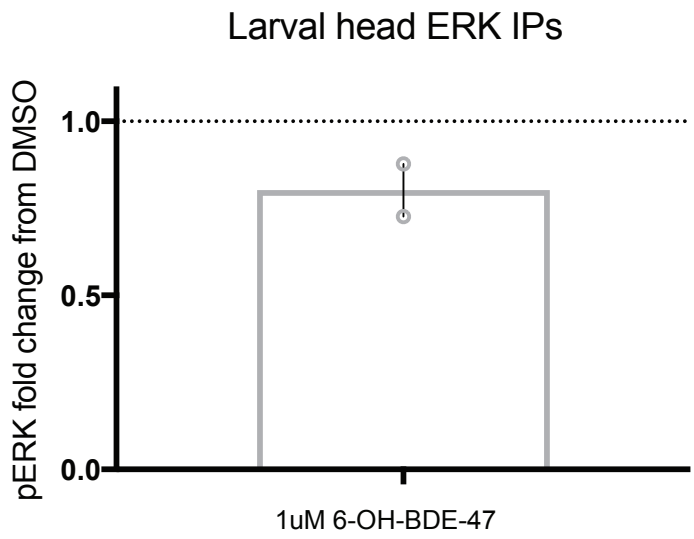

Poston et al. Supplementary Figure 4

Certain ortho-hydroxylated brominated ethers are promiscuous kinase inhibitors that impair neuronal signaling and neurodevelopmental processes

Robert G. Poston, Lillian Murphy, Ayna Rejepova, Mina Ghaninejad-Esfahani, Joshua Segales, Kimberly Mulligan, Ramendra N. Saha

Legends for supplemental figures

Supplemental Figure 1. Chronic PD0325901 exposure suppresses spontaneous neuronal activity. Primary embryonic rat cortical neurons grown on MEAs were chronically exposed to low doses of PD0325901, starting at the time of plating, in order to assess whether directly inhibiting MEK-ERK signaling would also affect spontaneous activity (in addition to regulating Bic-induced recurrent synchronous bursting (63)) and if it would produce similar effects as prolonged 6-OH-BDE-47 exposure. Detectable spontaneous activity was recorded and quantified across the first two weeks of growth *in vitro*, N=3. P-values generated with two-way ANOVA with post-hoc FDR method, Time $F(6,36) = 5.409$, P=0.0005, Treatment $F(2,36)=15.59$, $P<0.0001$, Interaction $F(12,36)=1.675$, P=0.1144.

Supplemental Figure 2. 6-OH-BDE-47 shares key structural features of non-ATP competitive type-III MEK1 inhibitors. (A) Chemical structures of the commercial MEK1 inhibitor PD0325901, BDE-47, and 6-OH-BDE-47 with key MEK-binding substituents highlighted. (B) Crystal structure of MEK1 (PDB: 3EQI) with top binding poses generated in ligand docking simulations for 6-OH and PD superimposed. (C) Rotated view of the allosteric binding pocket of MEK1 with most realistic generated poses of 6-OH and PD. We subsequently found that 6-OH does not inhibit MEK1 activity in a cell free kinase inhibition screen (Fig. 3). (D-E) Additional ligand-docking simulations conducted with CaMK1 (PDB IDs: 4FG7 (holo, ATP-bound CaMK1) and 4FGB (apo, non-ATP bound CaMK1), respectively). D. displays how the simulated interactions of 6-OH with CaMK1 cluster in the ATP-binding pocket, while in E., simulations conducted with the the apo form of CaMK1, where the binding pocket is in a non-ATP bound state, show that 6-OH binding does not localize to the ATP-binding pocket. This provides further evidence for the realistic nature of these binding predictions.

Supplemental Figure 3. Effects of acute environmentally relevant 6-OH-BDE-47 exposures. (A) Cells were acutely exposed to an estimated environmentally relevant exposure dose, 500nM, for increasing lengths of time before Bic+4AP stimulation (indicated as +B10') and whole-cell lysate collection, N=3-6. No significant 6-OH effects were detected. (B) To assess nuclear availability of pERK after 6-OH exposure, nuclear lysates were collected after 10 minute Bic+4AP treatment, N=4-5. P-values generated by one-way ANOVA with post-hoc LSD, Treatment $F(3,16)=7.491$, P=0.0024. (C) Acute 6-OH exposed cells were treated with either Bic+4AP or a lower concentration of Bic without 4AP to assess the effect of stimulus strength on nuclear availability of pERK, N=3. P-value generated by unpaired one-tailed t-test. All exposures noted as "chronic" are from the time of plating to the time of corresponding acute exposure experiments (conducted between DIV10 and 14).

Supplemental Figure 4. Additional Drosophila experimental timeline and data
(A) Detailed experimental timeline for Drosophila exposures and mushroom body axonal midline crossing assessment. (B) Representative western blot of ERK immune-precipitated from whole larval heads. Total ERK was precipitated from the pooled heads of ten DMSO and 6-OH exposed larvae. The fraction of pERK to total ERK was then determined by western blotting as a metric of MEK-ERK signaling *in vivo*. Quantification displayed in right panel. N=2 immuno-precipitations, each with n=10 exposed larval heads.